Molecular and Cellular Endocrinology 382 (2014) 938–949

Contents lists available at ScienceDirect

Molecular and Cellular Endocrinology

journal homepage: www.elsevier.com/locate/mce

Real-time trafficking and signaling of the glucagon-like peptide-1 receptor

Sarah Noerklit Roed [a,e,*], Pernille Wismann [a], Christina Rye Underwood [a], Nikolaj Kulahin [a], Helle Iversen [a], Karen Arevad Cappelen [a], Lauge Schäffer [b], Janne Lehtonen [c], Jacob Hecksher-Soerensen [c], Anna Secher [c], Jesper Mosolff Mathiesen [d], Hans Bräuner-Osborne [d], Jennifer L. Whistler [e], Sanne Moeller Knudsen [a], Maria Waldhoer [a]

[a] Department of Incretin & Islet Biology, Novo Nordisk A/S, Maaloev, Denmark
[b] Department of Diabetes Protein Engineering, Novo Nordisk A/S, Maaloev, Denmark
[c] Department of Histology and Imaging, Novo Nordisk A/S, Maaloev, Denmark
[d] Department of Drug Design and Pharmacology, Faculty of Health and Medical Sciences, University of Copenhagen, Copenhagen, Denmark
[e] Ernest Gallo Clinic and Research Center, Department of Neurology, University of California San Francisco, San Francisco, USA

ARTICLE INFO

Article history:
Received 28 April 2013
Received in revised form 8 November 2013
Accepted 16 November 2013
Available online 22 November 2013

Keywords:
Seven transmembrane-spanning receptors/
G protein-coupled receptors
Glucagon-like peptide-1
Trafficking
cAMP signaling
Fluorescent microscopy
Real-time TR-FRET

ABSTRACT

The glucagon-like peptide-1 incretin receptor (GLP-1R) of family B G protein-coupled receptors (GPCRs) is a major drug target in type-2-diabetes due to its regulatory effect on post-prandial blood-glucose levels. The mechanism(s) controlling GLP-1R mediated signaling are far from fully understood. A fundamental mechanism controlling the signaling capacity of GPCRs is the post-endocytic trafficking of receptors between recycling and degradative fates. Here, we combined microscopy with novel real-time assays to monitor both receptor trafficking and signaling in living cells. We find that the human GLP-1R internalizes rapidly and with similar kinetics in response to equipotent concentrations of GLP-1 and the stable GLP-1 analogues exendin-4 and liraglutide. Receptor internalization was confirmed in mouse pancreatic islets. GLP-1R is shown to be a recycling receptor with faster recycling rates mediated by GLP-1 as compared to exendin-4 and liraglutide. Furthermore, a prolonged cycling of ligand-activated GLP-1Rs was observed and is suggested to be correlated with a prolonged cAMP signal.

1. Introduction

GLP-1[1] is a key incretin hormone that regulates post-prandial blood glucose levels. GLP-1 is secreted from the intestinal L-cells in response to food intake and activates the 7TM[2]/GPCR[3] GLP-1R[4] located on e.g. pancreatic β-cells. Activated GLP-1R then initiates several effects leading to an overall decrease in blood glucose levels, including i) increased insulin secretion in a glucose-dependent manner, an effect commonly known as the incretin effect, ii) decreased glucagon secretion, and iii) decreased food intake through satiety induction (Holst, 2007). These effects are diminished in type 2 diabetic patients, which has led to the development of GLP-1R agonists as anti type-2-diabetic drugs (Meier and Nauck, 2010). Since endogenous GLP-1 is quickly degraded by dipeptidyl peptidase-4 (DPP-4[5]) and cleared by the kidneys, long-acting GLP-1 analogues are used for treatment purposes. Two such analogues have been approved, exenatide and liraglutide (Meier, 2012).

The signaling cascades leading to insulin secretion via GLP-1R have been extensively studied (Mayo et al., 2003). However, the mechanism(s) involved in the termination of GLP-1R-mediated cellular processes remain largely unknown (Widmann et al., 1996a,b, 1997). One highly conserved mechanism that is important for terminating G protein-mediated signaling from many 7TM/GPCRs is the internalization/endocytosis and the subsequent intracellular sorting of the receptors. Specifically, following activation by a ligand, many 7TM/GPCRs are phosphorylated by GPCR kinases, bind β-arrestins and are internalized (Hanyaloglu and von Zastrow, 2008). Internalized receptors are then either recycled back to the

* Corresponding author. Address: Department of Incretin & Islet Biology, Novo Nordisk A/S, Novo Nordisk Park, 2760 Maaloev, Denmark. Tel.: +45 30759317.
E-mail address: snro@novonordisk.com (S.N. Roed).

[1] Glucagon-like peptide-1.
[2] Seven transmembrane-spanning.
[3] G protein-coupled receptor.
[4] Glucagon-like peptide-1 receptor.
[5] Dipeptidyl peptidase-4.

0303-7207
http://dx.doi.org/10.1016/j.mce.2013.11.010

cell surface where they can engage with ligands once again, or targeted for post-endocytic degradation, resulting in permanent signal termination from the receptor (Tsao et al., 2001; Whistler et al., 2002).

Both the rat and the human GLP-1Rs have been shown to rapidly internalize after activation by GLP-1 (Widmann et al., 1995; Jorgensen et al., 2007; Kuna et al., 2013). However, the kinetics of internalization as well as the post-endocytic sorting of GLP-1Rs in response to diverse ligands – including approved drugs – have not yet been studied in detail.

Here, we investigated the internalization and the signaling capacity of GLP-1R in real time in living cells using FRET[6] techniques in response to GLP-1, exendin-4 and liraglutide. In addition, we monitored the post-endocytic fate of GLP-1R and its ligands as well as confirmed the biological relevance of GLP-1R internalization in vivo using fluorescently labeled GLP-1 analogues.

2. Experimental procedures

2.1. Materials

Cell culture medium (DMEM) with glutaMAX™-I and 4.5 g/L D-glucose, Dulbecco's phosphate-buffered saline (DPBS) without $CaCl_2$ and $MgCl_2$, optimem®I with glutaMAX™-I, lipofectamine2000, hank's balanced salt solution (HBSS), alexa fluor® 594 goat anti-mouse $IgG_1(\gamma1)$ (IgG_1-594), geneticin, fetal bovine serum (FBS), transferrin from human serum alexa fluor 594 conjugate, 4–12% bis-tris gels, invitrolon PVDF/filter paper, rprotein-G sepharose 4B conjugate beads, 20× MOPS SDS running buffer and 20× transfer buffer were purchased from Invitrogen (Naerum, Denmark). N-terminally SNAP-tagged human GLP-1R construct (SNAP-GLP-1R), SNAP-tagged β_2AR construct (SNAP-β_2AR), tag-lite® SNAP lumi4®-Tb (terbium energy donor), tag-lite internalization reagent (energy acceptor), and SNAP/CLIP lab medium 5× were purchased from Cisbio Bioassays (Codolet, France). LANCE/DELFIA D400 and CFP/YFP (D450_515) single mirrors, excitation filters X340_101 and CFP-430 (X430), emission filters 520/8, M615_203, CFP-470 (M470), and YFP-535 (M535), and sterile and tissue culture treated white opaque 96-well microplates were purchased from Perkin Elmer (USA). ECM gel from engelbreth-holm-swarm mouse sarcoma, poly-D-lysine hydribromide, tris base, $CaCl_2$, $MgCl_2$, HEPES, tween20, L-gluthathione reduced, iodoacetamide, albumin from bovine serum, Tris-Cl and isoproterenol were purchased from Sigma Aldrich (Broendby, Denmark). NaCl and KCl were purchased from Merck (Whitehouse Station, USA). NaOH and EZ-link sulfo-NHS-SS-biotin were purchased from Thermo Fisher Scientific (USA). Human embryonic kidney cells (HEK293) were purchased from ATTC (Boras, Sweden). C57BL6 mice were purchased from Taconic. SNAP-surface® alexa fluor® 488 (SNAP-substrate-488), PNGase F cocktail and rabbit polyclonal SNAP-tag antibody were purchased from New England Biolabs (Ipswich, USA). Paraformaldehyde (PFA) and OCT were purchased from VWR Bie & Berntsen (Herlev, Denmark). Vectorshield mounting medium with DAPI and Vectastain ABC Kit peroxidase standard PK-4000 were purchased from Vector Laboratories (Burlingame, USA). Faramount mounting media was purchased from DAKO. Lumigen PS3 detection reagent was purchased from GE Healthcare (USA). Sotalol was purchased from Tocris Bioscience (UK). 8-well permanox lab-tek® chamber slides™ were purchased from NUNC (Roskilde, Denmark). Black 384 tissue culture treated plates were purchased from BD Falcon (USA). Complete protease inhibitor cocktail tablets were purchased from Roche Diagnostics (Indianapolis, USA). All unlabeled GLP-1R ligands were prepared in house using standard methods.

2.2. Synthesis of fluorescently labeled ligands

For visualization of GLP-1R ligands, GLP-1, exendin-4, exendin9-39 and liraglutide were synthetically labeled with red fluorophores or VivoTag750. N-alpha-Fmoc-[Arg26,Arg34,Lys37]-GLP-1 (GLP-1-synth) was synthesized on Fmoc-Lys-Wang resin whilst N-alpha-Fmoc-[Leu14,Arg27,Leu28]-exendin-4 (exendin-4-synth), [Leu14,Leu28]-exendin-4-Cys-amide (exendin-4C-synth), [Leu14,-Leu28]-exendin9-39-Cys-amide (exendin9-39-synth), and liraglutide-Cys-amide (liraglutide-synth) were synthesized on PAL or Rink ChemMatrix resin by standard Fmoc chemistry using a Liberty peptide synthesizer. After purification by RP-HPLC, 2 μmol of GLP-1-synth and exendin-4-synth were reacted with 1 mg Alexa594-NHS in 200 μl DMSO and 2 μl triethylamine for 2 h. Following, 4 μl of piperidine were added, and after 10 min the Fmoc protecting group was completely removed. For liraglutide, 2 μmol of liraglutide-synth was reacted with 1 mg Alexa594-maleimide in 200 μl DMSO and 2 μl collidine for 2 h. For exendin-4(VivoTag750) and exendin9-39(VivoTag750), 0.7 μmol of exendin-4C-synth or exendin9-39-synth were reacted with 1 mg VivoTag750-maleimide in 100 μl DMSO and 2 μl collidine for 30 min. N-epsilon37-Alexa594-[Arg26,Arg34,Lys37]-GLP-1 (referred to as GLP-1-594), N-epsilon12-Alexa594-[Leu14,Arg27,Leu28]-exendin-4 (referred to as exendin-4-594), and liraglutide-Cys(Alexa594)-amide (referred to as liraglutide-594) were purified by RP-HPLC and their theoretical masses of 4189, 4902, and 4742 Da, respectively, were confirmed by mass spectrometry. For exendin-4-cys(VivoTag750)-amide (referred to as exendin-4-VT750) and exendin9-39-cys(VivoTag750)-amide (referred to as exendin9-39-VT750), 200 μl 20 mM ammonium bicarbonate was added and the peptides purified using a PD-10 column eluted with 20 mM ammonium bicarbonate. The labeled peptides eluted first and were collected in 1.2 ml eluate and lyophilized. The fluorescent labeling of liraglutide does not alter the binding properties to GLP-1R, whilst the binding affinities of GLP-1-594 and exendin-4-594 change marginally compared to unlabeled ligands (Supplementary Fig. 1).

2.3. SNAP-tagging of GLP-1R

For visualization of GLP-1R, a SNAP-tag epitope was fused to the extracellular N-terminus of the human GLP-1R (Cisbio Bioassays, 2012). The SNAP-tag is a derivative of O6-guanine nucleotide alkyltransferase, which can covalently react with e.g. fluorescent-conjugated benzyl guanine substrates (Maurel et al., 2008). The N-terminal SNAP-tag on GLP-1R does not alter the binding properties of GLP-1 to the receptor (Supplementary Fig. 2).

2.4. Cell culture

To generate a cell line stably expressing the SNAP-GLP-1R HEK293 (referred to as SNAP-GLP-1R cells), HEK293 cells were transfected with the SNAP-GLP-1R plasmid using Lipofectamine2000. In addition, a HEK293 cell line stably expressing both the SNAP-GLP-1R and the EPAC[7] cAMP sensor with mCerulean and mCitrine as FRET pair as described previously (Mathiesen et al., 2013) was also generated (referred to as GLP-1R-EPAC cells). Cells were maintained in DMEM supplemented with 10% heat-inactivated FBS and 0.8 mg/ml geneticin for selection of positive clones in a humidified 5% CO_2 air incubator at 37 °C.

2.5. Real Time cAMP signaling assay using an EPAC-sensor

GLP-1R-EPAC cells were seeded in sterile, black 384-well microplates coated with ECM and cultured overnight. Cells were

[6] Fluorescence Resonance Energy Transfer.

[7] Exchange protein activated by cAMP.

incubated in HBSS buffer (20 mM HEPES supplemented with 1 mM $CaCl_2$, 1 mM $MgCl_2$, and 0.02% Tween20) in darkness for 10 min prior to stimulation with ligands in the concentrations indicated at room temperature. To measure the effect of receptor inactivation on cAMP signaling, 10 μM of the GLP-1R antagonist exendin9-39 was added following 20 min of agonist stimulation. Increases in the mCerulean/mCitrine ratio reflecting increasing cAMP levels were measured using an Envision 2104 Multilabel Reader (Perkin Elmer, USA). Excitation of the EPAC donor (mCerulean) was performed using a CFP/YFP (D450_515) single mirror and an excitation optical filter CFP-430 (X430). Emission was recorded using CFP-470 (M470) and YFP-535 (M535) filters, respectively. mCerulean/mCitrine ratios were plotted as a function of time. EC_{50} values were calculated from concentration-response curves with area under the curve (AUC) vs. ligand concentrations plotted in GraphPad Prism 5.03 Software (San Diego, California, USA).

2.6. Immunocytochemistry and confocal microscopy

SNAP-GLP-1R cells were seeded in 8-well chamber slides coated with ECM gel and cultured for 24 h. Surface expressed SNAP-GLP-1Rs were labeled by incubation with 5 μM SNAP-substrate-488 diluted in DMEM for 30 minutes at 37 °C and 5% CO_2 followed by a washing step with PBS. ***Internalization assays*** – Cells were stimulated with 100 nM of fluorescently labeled ligands at 37 °C for the time periods indicated. ***Co-localization experiments with transferrin –*** Cells were serum starved for 60 min prior to the experiment and surface expressed receptors were labeled with the SNAP-substrate-488 for the last 30 min of starvation. Next, the cells were washed in PBS and receptor internalization was induced by incubation with 100 nM unlabeled ligands at 37 °C for the time periods indicated. Finally, internalized receptors were traced to the recycling endosomes by incubation of the cells with alexa fluor 594-conjugated transferrin (1:500) for the last 15 minutes of ligand incubation. Cells were washed in PBS, fixed in 4% PFA for 20 minutes at 37 °C and mounted in Vectashield-DAPI mounting medium. ***Confocal Microscopy*** – The labeled proteins and peptides were visualized using a Zeiss LSM 510 Meta confocal microscope (Birkeroed, Denmark) equipped with 405 nm, 488 nm, and 543 nm excitation lasers, using a 40× 1.3 NA oil immersion objective. Images were processed using the Zen lite 2011 software (Carl Zeiss MicroImaging GmbH) and Adobe Photoshop CS3.

2.7. GLP-1R internalization in mouse pancreas

C57BL6 mice were injected IV with 120 nmol/kg exendin-4-VT750 or exendin9-39-VT750. After 6 h the mice were sacrificed and perfusion fixed with heparinized (10U/ml) saline (2 × 5 ml) followed by Neutral buffered formalin (NBF; 2 × 5 ml). The pancreata were removed and fixed in NBF overnight. The next day the tissue was incubated for 6 h in 30% sucrose in PBS and subsequently transferred to a plastic mould, covered with OCT and frozen by placing the mould on a block of dry ice. The frozen blocks were cut into 10 μm sections on a cryostat (Leica) and mounted on slides. For long term storage the slides were kept at −80 °C. To visualize the exendin-4/exendin9-39 signal in the islets the frozen sections were transferred to room temperature for 10 min. Residual OCT media was removed by washing 3 times five minutes in PBS. The slides were mounted in Faramount mounting media and pictures were taken using a 10× objective on an Olympus microscope BX53 fitted with a Neo sCMOS camera (Andor Technology). All in vivo experiments were performed in accordance with animal licence number 2012-15-2934-00135.

2.8. TR-FRET based real-time receptor internalization assay

A TR-FRET[8] based assay was performed for GLP-1R internalization studies in real-time (Fig. 1 (Cisbio Bioassays, 2012)). SNAP-GLP-1R cells were seeded in sterile, white 96-well microplates coated with ECM and cultured overnight. Surface expressed SNAP-GLP-1Rs were labeled with 100 nM tag-lite® SNAP Lumi4®-Tb in OptiMem for 60 min at 37 °C. This Tb-labeling of SNAP-GLP-1R did not influence the ligand binding to the receptor (Supplementary Fig. 3). Subsequently, cells were washed in SNAP/CLIP lab medium (1:5) and incubated in preheated tag-lite internalization reagent (1:20, 37 °C). Cells were stimulated with preheated ligands in the concentrations indicated and the plate was read in an Envision 2104 Multilabel Reader (Perkin–Elmer, USA). The reading chamber was maintained at 37 °C throughout the entire reading time. Excitation of the SNAP Lumi4®-Tb was performed using a LANCE/DELFIA D400 single mirror and an excitation optical filter X340_101. Emission was measured using M615_203 and 520/8 emission filters. The acceptor and donor emission signals were measured every 6 min. Receptor internalization was assessed by calculating the ratio between the donor (=SNAP-GLP-1Rs) vs. the acceptor emission (=tag-lite internalization reagent present in extracellular medium, for details see Fig. 1) and the results were fitted using a product of one phase association and one phase decay models using GraphPad Prism. Concentration-response curves were generated using the donor/acceptor ratios at 20 min. ***TR-FRET based real-time recycling assay –*** 20 or 90 min following initial agonist addition, 10 μM of exendin9-39 was added to stop further receptor internalization and to trap any recycled receptors on the cell surface (Martini et al., 2007) (Fig. 1C). Donor/acceptor ratios were plotted as a function of time and the results were fitted using a one-phase association model (internalization phase) and a one-phase decay model (recycling phase). ***TR-FRET based real-time internalization and recycling assays with β_2AR*** – HEK293 cells were transiently transfected with SNAP-β_2AR plasmids using Lipofectamine2000. Real-time internalization and recycling assays were performed by stimulating the transfected cells with the agonist isoproterenol and the antagonist sotalol as described above.

2.9. Biotinylation protection degradation assay

The experiment was carried out essentially as previously described (Martini et al., 2007;Tschische et al., 2010). In brief, SNAP-GLP-1R cells were incubated with disulphide cleavable biotin for 30 min at 4 °C and washed with TBS (137 mM NaCl, 25 mM tris-base, 3 mM KCl, 1 mM $CaCl_2$, pH 7.4). Cells were then equilibrated in DMEM for 30 min at 37 °C prior to stimulation with 100 nM of either GLP-1, exendin-4, liraglutide or vehicle (DMEM) at 37 °C for the time periods indicated to allow receptor endocytosis and recycling/degradation. Remaining cell surface-biotin was stripped (50 mM glutathione, 75 mM NaCl and 10% FBS) (except 100% plates) and quenched (50 mM iodoacetamide, 10% BSA in PBS), followed by cell lysis (0.1% triton X-100, 150 mM NaCl, 25 mM KCl, 10 mM Tris–HCl, 1 mM $CaCl_2$, 5 mM iodoacetamide, pH 7.4, with complete protease inhibitors). Samples were immunoprecipitated with SNAP-tag antibody o/n at 4 °C followed by 60 min incubation with protein-G sepharose beads at 4 °C. Precipitates were washed, deglycosylated, resolved by SDS/PAGE and visualized with Vectastain ABC. Four independent blots were analyzed using ImageJ 1.45s Software and quantified with 15 min samples designated as 100%. Degradation rates were calculated by fitting to a one-phase decay model.

[8] Time-Resolved Fluorescence Resonance Energy Transfer.

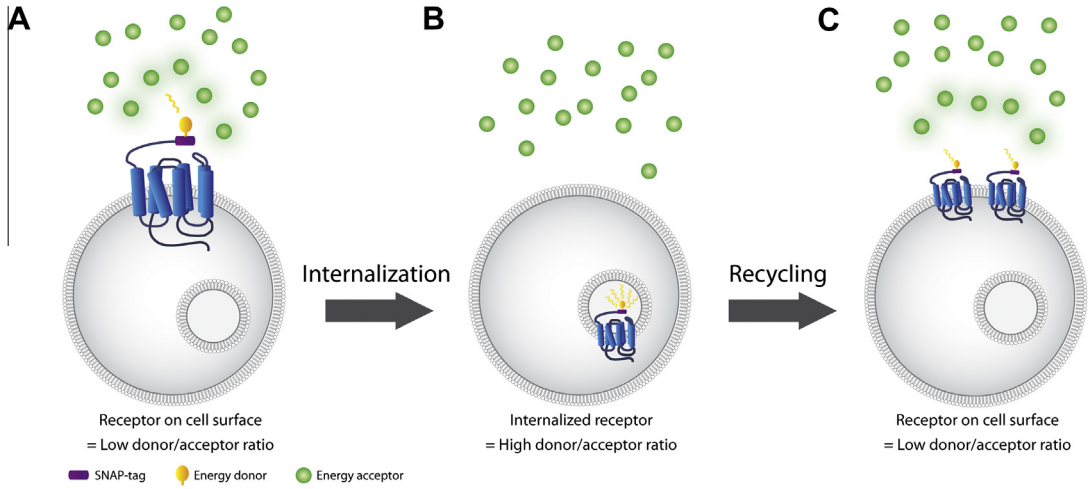

Fig. 1. Illustration of the TR-FRET based real-time internalization technique. Surface expressed SNAP-tagged receptors are labeled with a cell-impermeable tag-lite® SNAP Lumi4®-Tb (= energy donor, yellow). Then cells are incubated in excess of cell-impermeable tag-lite internalization reagent (= energy acceptor, green dots). **(A)** Excitation of the donor results in energy transfer from the donor to the acceptor, resulting in a high TR-FRET signal. Due to the excess amount of acceptor, the donor emission is quenched, thereby resulting in an overall low donor/acceptor ratio. **(B) Receptor internalization**. Ligand induced receptor internalization results in an increased distance between the donor and the acceptor subsequently exceeding the limits for energy transfer (= decreased TR-FRET signal). Simultaneously, the now intracellular donor is no longer quenched by the acceptor resulting in an overall increased donor/acceptor ratio. **(C) Receptor Recycling**. Receptor recycling results in re-surfacing of the donor, which is resituated in close proximity to the acceptor (= overall low donor/acceptor ratio). Modified from Cisbio Bioassays (Cisbio Bioassays, 2012).

2.10. Statistical analysis

Statistical analyses were performed using one-way ANOVA analysis of variance followed by a Tukey's post-test for comparisons between multiple groups in GraphPad Prism. Dunnett' post-test was used for comparisons of sample groups to a control group. $P < 0.05$ was considered statistically significant.

3. Results

3.1. Rapid and prolonged agonist induced GLP-1R mediated cAMP production

The signaling cascades downstream of ligand-activated GLP-1R leading to insulin secretion involve a rapid elevation of cAMP through stimulation of $G\alpha_s$ proteins (Holst, 2007). We first set out to investigate the kinetics of GLP-1R signaling in response to various agonists utilizing an EPAC cAMP FRET-sensor (Ponsioen et al., 2004; Mathiesen et al., 2013). GLP-1R-EPAC cells were stimulated with either the human natural incretin hormone GLP-1 (Fig. 2A), or one of the two DPP-4 cleavage-resistant GLP-1R agonists, exendin-4 (Fig. 2B) and liraglutide (Fig. 2C). Upon stimulation with GLP-1, the GLP-1R mediated cAMP production reflected by the mCerulean/mCitrine ratio increased immediately in a concentration-dependent manor resulting in a stable plateau for [GLP-1] > 10 pM. This plateau was maintained for a minimum of 3 h in this assay setup (Fig. 2A). Likewise, stimulation with either exendin-4 (Fig. 2B) or liraglutide (Fig. 2C) resulted in a fast and prolonged cAMP production. No significant differences in maximum response nor potency were found comparing the three ligands, with EC_{50} being 9.8 ± 1.0 pM, 23 ± 10 pM and 36 ± 10 pM for GLP-1, exendin-4 and liraglutide, respectively. The effect of receptor inhibition on cAMP signaling was measured by adding an excess of 10 μM of the GLP-1R antagonist exendin9-39 (Göke et al., 1993) following 20 min of agonist stimulation. The cAMP signal decreased to basal levels following addition of exendin9-39 for all three agonists tested (Fig. 2D–F). Only at the highest agonist concentration the antagonist was not sufficient to compete for binding to the GLP-1R (agonist/antagonist ratio 1:1000) and, as a consequence, failed to silence the cAMP signal.

In summary, real-time cAMP production of GLP-1R in response to all agonists tested revealed an equally rapid and prolonged cAMP signal, which could be reversed upon the addition of excess of antagonist.

3.2. Visualization of both GLP-1R and ligand internalization in living cells

Typically, signaling from 7TM/GPCRs is terminated by a highly conserved cascade of events, involving receptor phosphorylation by GRKs, subsequent β-arrestin recruitment and receptor internalization. These processes are commonly known to contribute directly to the rapid desensitization of 7TM/GPCRs by facilitating the uncoupling of the receptor from its G-protein, whilst recycling is thought to contribute to receptor resensitization (Hanyaloglu and von Zastrow, 2008). Both the rat and human GLP-1Rs have previously been suggested to rapidly internalize following activation with radiolabeled GLP-1 (Widmann et al., 1995; Jorgensen et al., 2007). However, in these studies, receptor internalization was inferred indirectly, i.e. by monitoring the internalization of the ligand.

Here, we simultaneously monitored the internalization properties of both GLP-1R and agonists in living SNAP-GLP-1R cells. For visualization of the receptor, the surface-expressed SNAP-GLP-1Rs were labeled with the fluorescent cell impermeable SNAP-substrate-488 (Fig. 3A and C–E, green). Then cells were stimulated with 100 nM of either GLP-1-594 (Fig. 3A–C, red), exendin-4-594 (Fig. 3D, red), or liraglutide-594 (Fig. 3E, red) for the time periods indicated to induce receptor internalization. Both the SNAP-GLP-1Rs (Fig. 3A) and GLP-1-594 (Fig. 3B) rapidly internalized and co-localized in intracellular vesicles as soon as 5 min post stimulation (Fig. 3C, yellow merge). Stimulation of the SNAP-GLP-1R with exendin-4-594 (Fig. 3D) likewise induced a rapid internalization of GLP-1Rs whilst stimulation with liraglutide-594 (Fig. 3E) resulted in a slightly delayed internalization when compared to GLP-1 (compare 5 and 15 min points). Nevertheless, in the case

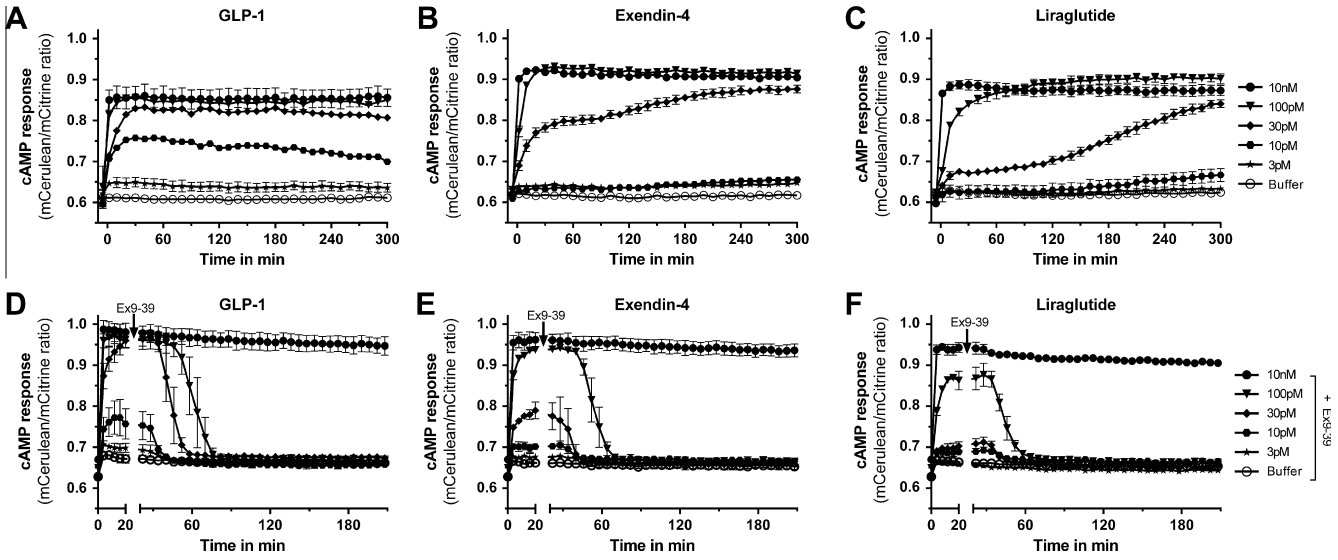

Fig. 2. Real-time GLP-1R induced cAMP production. GLP-1R-EPAC cells were stimulated with increasing concentrations of ligands and cAMP production was measured in real-time at room temperature. Real-time GLP-1R cAMP production induced by **(A)** GLP-1, **(B)** exendin-4, or **(C)** liraglutide, reflected by an increase in the mCerulean/mCitrine ratio and plotted as a function of time. Decrease in cAMP production in response to GLP-1R inhibition by addition of 10 μM exendin9-39 after 20 min stimulation (indicated by arrow) with **(D)** GLP-1, **(E)** exendin4, or **(F)** liraglutide. Data represent mean ± SD from one representative out of three independent experiments carried out in triplicates.

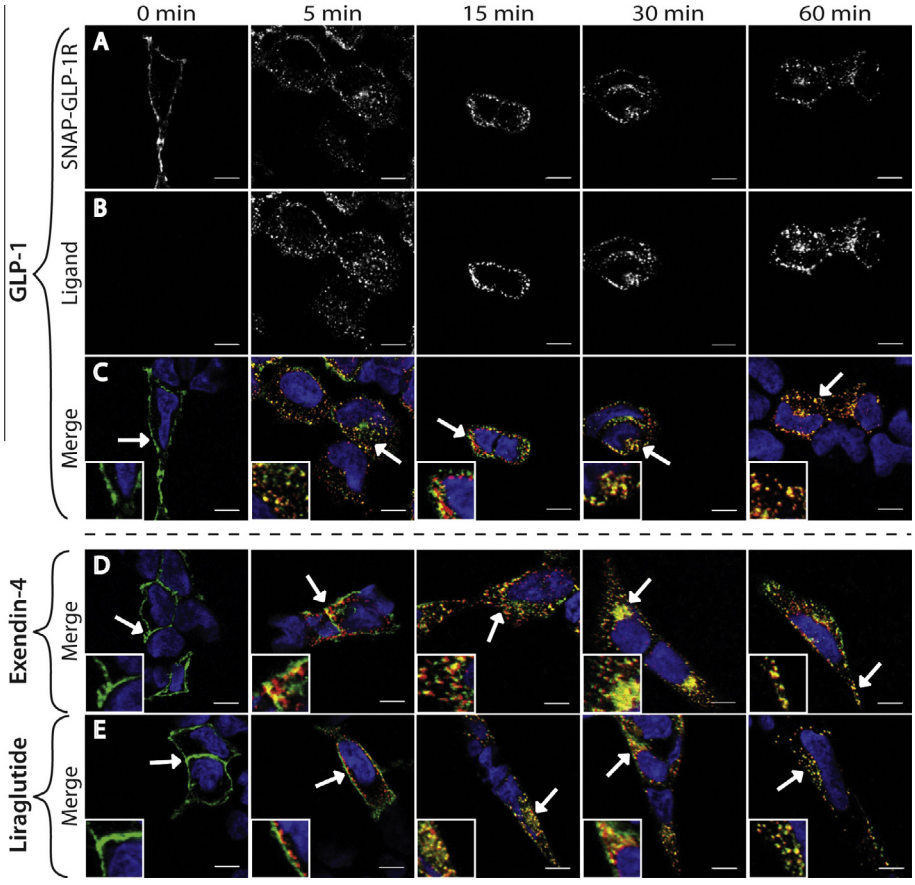

Fig. 3. Internalization of GLP-1Rs with fluorescently labeled ligands. Surface expressed SNAP-GLP-1Rs were labeled with a cell-impermeable SNAP-substrate-488 and cells were subsequently stimulated with 100 nM of fluorescently labeled ligands for the time periods indicated. **(A)** SNAP-GLP-1Rs internalize in the presence of **(B)** GLP-1-594. Merged pictures of SNAP-GLP-1Rs (green) in the presence of **(C)** GLP-1-594, **(D)** exendin-4-594, or **(E)** liraglutide-594. Co-localization (yellow), DAPI (blue), magnifications as indicated by arrow (insert). Scale bars = 10 μm. Pictures are representatives from three independent experiments.

of all three ligands, both receptor and ligands were observed to co-localize intracellularly for up to 60 min.

In summary, GLP-1, exendin-4 and liraglutide all induced a rapid internalization of the SNAP-GLP-1R and co-localized with the receptor for up to 60 minutes in intracellular compartments.

3.3. GLP-1R internalization in vivo in mouse pancreatic islets

As shown in HEK293 cells (Fig. 3), the GLP-1R internalizes concomitantly with agonists and this agonist-receptor complex remains intact within the cell for a prolonged period of time. For instance, exendin-4 (Fig. 3D) can be observed in complex with GLP-1R for a minimum of 60 min following receptor stimulation. We hence set out to verify that exendin-4 promotes GLP-1R internalization in vivo in a relevant tissue, such as mouse pancreatic islets. Living C57BL6 mice were injected IV with 120 nmol/kg fluorescently labeled exendin-4-VT750 or exendin9-39-VT750 followed by formalin perfusion of the sacrificed animal, isolation of the pancreas and preparation of slides of whole pancreas for microscopy (Fig. 4). Exendin-4-VT750 was detected in intracellular clusters in a pancreatic islet, suggesting that the GLP-1R readily internalizes in the presence of exendin-4 in vivo (Fig. 4A). Upon injection of mice with the antagonist exendin9-39-VT750, no internalization of the GLP-1R was observed. Instead, the fluorescence labeling was confined exclusively to the plasma membrane, suggesting that – in the presence of an antagonist – GLP-1Rs are located on the cell surface (Fig. 4B). As a control, exendin4-bound GLP-1Rs were shown to localize intracellularly in insulin-positive pancreatic β-cells, thereby further confirming the internalization of GLP-1R in its native environment (Supplementary Fig. 4).

These data confirm that GLP-1R internalization is a biological phenomenon occurring both in a recombinant HEK293 cell line as well as in pancreatic islets.

3.4. Post-endocytic sorting of GLP-1Rs to early recycling endosomes

Following internalization, 7TM/GPCRs can have different fates, i.e. receptors can i) be recycled back to the cell surface, ii) reside in endosomes, or iii) be transported for degradation in e.g. lysosomes (Hanyaloglu and von Zastrow, 2008). Thus, we next examined the post-endocytic fate of internalized GLP-1Rs following prolonged ligand stimulation.

It was previously reported that GLP-1R recycles after internalization (Widmann et al., 1995). Hence, we tested whether the SNAP-GLP-1R redistributes to early recycling endosomes and co-localizes with the recycling endosomal marker transferrin (Grant and Donaldson, 2009). Receptor internalization was first induced by stimulation with 100 nM of unlabeled ligand for the time periods indicated. Following, receptor co-localization with early recycling endosomes was visualized by labeling the endosomes with alexa594-conjugated transferrin for the final 15 min of the experiment. A profound co-localization of the SNAP-GLP-1R (Fig. 5A) with transferrin (Fig. 5B) was observed following stimulation with GLP-1 (Fig. 5C, yellow merge). Receptors were found in transferrin positive endosomes up to 45 min post-ligand addition. In the presence of exendin-4 (Fig. 5D) and liraglutide (Fig. 5E), co-localization of internalized SNAP-GLP-1R and transferrin was observed for up to 60 min following ligand addition.

These data suggest that, following agonist induced internalization, GLP-1Rs pass through early recycling endosomes and – in the presence of exendin-4 and liraglutide – recycling endosomal localization was observed up to 60 min post-stimulation.

3.5. Real-time internalization of GLP-1R in living cells

To further characterize the dynamics of both GLP-1R internalization and recycling in response to various ligands and ligand concentrations in real time, we conducted a novel TR-FRET based receptor internalization assay (Fig. 1 (Cisbio Bioassays, 2012)). Surface expressed SNAP-GLP-1Rs were labeled with tag-lite® SNAP lumi4®-Tb (=energy donor) and cells were incubated in the cell-impermeable tag-lite internalization reagent (=energy acceptor). Receptor internalization was induced by stimulation with increasing concentrations of GLP-1 (Fig. 6A), exendin-4 (Fig. 6B), or liraglutide (Fig. 6C). For all ligands, GLP-1R internalization was fast and concentration-dependent with equal maximal internalization levels (Fig. 6A–C). The potency of GLP-1 (EC_{50} of 12.0 ± 4.84 nM) and exendin-4 (EC_{50} of 13.1 ± 3.56 nM) for inducing GLP-1R internalization were significantly higher when compared to liraglutide (EC_{50} of 158 ± 21.6 nM) (Fig. 6D). Interestingly, when comparing the GLP-1R internalization rate at the EC_{50} concentration for each ligand, no significant differences were observed for the three ligands with $t_{1/2\_int}$ of 11.6 ± 0.8 min for GLP-1 (at 10 nM, Fig. 6A), $t_{1/2\_int}$ of 21.1 ± 1.7 for exendin-4 (at 10 nM, Fig. 6B), and $t_{1/2\_int}$ of 16.5 ± 2.0 for liraglutide (at 100 nM, Fig. 6C) (Table 1). For all ligands, stimulation with high agonist concentration, i.e. 1 μM, resulted in a maximum GLP-1R internalization level within 15–20 min. This maximum internalization level was followed by

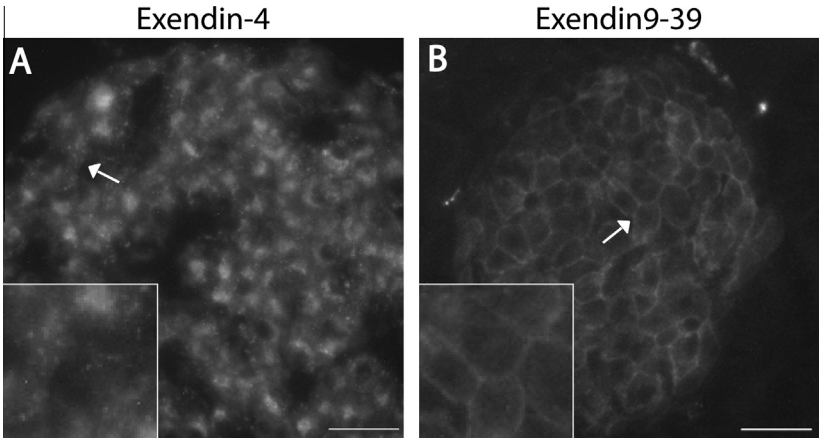

Fig. 4. GLP-1R internalization in mouse pancreatic islets. Living C57BL6 mice were injected IV with 120 nmol/kg fluorescently labeled **(A)** exendin-4-VT750 or **(B)** exendin9-39-VT750 followed by formalin perfusion of the sacrificed animal, isolation of the pancreas and preparation of slides of whole pancreas for microscopy. **(A)** Clusters of the agonist exendin-4-750 detected intracellularly in a pancreatic islet. **(B)** Cell membrane labeling in a pancreatic islet after injection with exendin9-39-750. Magnifications as indicated by arrow (insert). Scale bars = 100 μm. Pictures are representatives from pancreatic slides prepared from two mice.

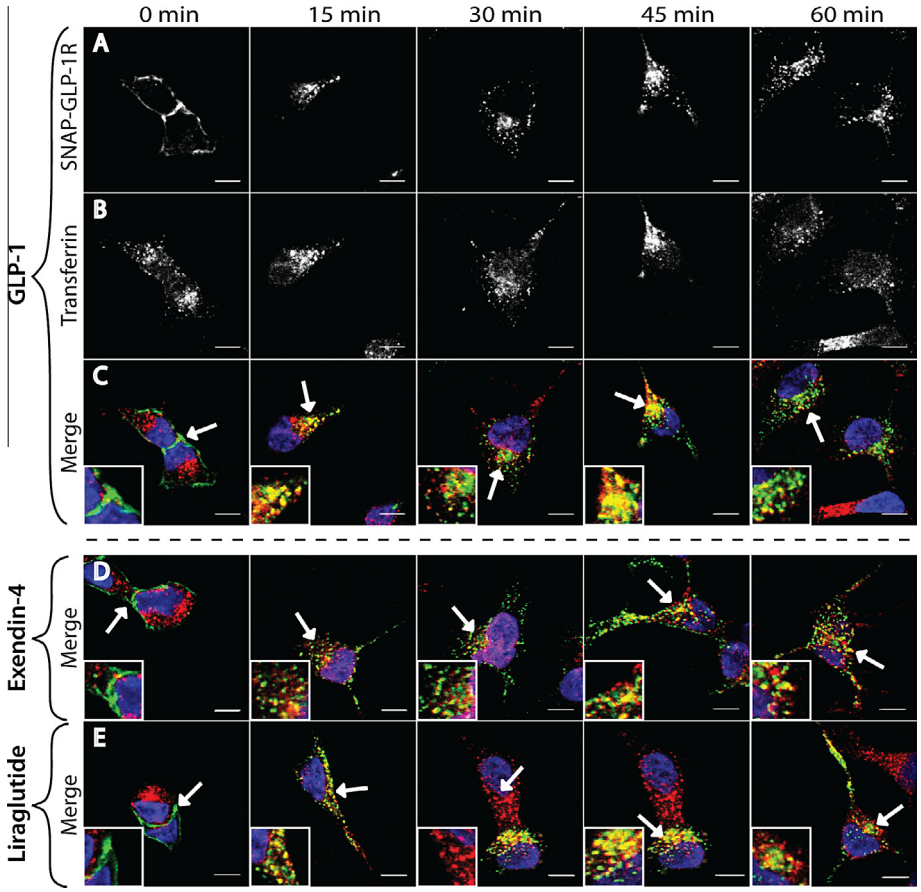

Fig. 5. Internalized GLP-1Rs co-localize with early recycling endosomes. Surface expressed SNAP-GLP-1Rs were labeled with a cell-impermeable SNAP-substrate-488 and cells were subsequently stimulated with 100 nM of ligands for the time points indicated. The early recycling endosomes were labeled with Transferrin-594 for the last 15 min of the experiment. **(A)** GLP-1 stimulated SNAP-GLP-1Rs in the presence of **(B)** transferrin-stained early recycling endosomes. Merged pictures of SNAP-GLP-1Rs (green) in the presence of **(C)** GLP-1, **(D)** exendin-4, or **E)** liraglutide and early recycling endosomes (red). Co-localization (yellow), DAPI (blue), magnifications as indicated by arrow (insert). Scale bars = 10 μm. Pictures are representatives from three independent experiments.

a plateau, which only marginally decreased over the 60 min time period of the assay (Fig. 6A–C).

These data show that GLP-1R internalizes rapidly and – importantly – at similar rates in response to all ligands tested. GLP-1 and exendin-4, however, were 10-fold more potent than liraglutide to induce GLP-1R internalization.

3.6. Real-time recycling of GLP-1R

In our microscopy studies, we could observe a significant amount of internalized GLP-1Rs in recycling endosomes for all ligands tested (see Fig. 5). Thus, we next examined the recycling kinetics of GLP-1R in real time by adding an excess of exendin9-39 at the time point of maximum agonist induced GLP-1R internalization (~20 min post agonist stimulation, Fig. 7A–C, arrows). Using this experimental approach, we anticipated recycling to be reflected in a decreased donor/acceptor ratio, since the internalized donor-labeled GLP-1Rs should – upon re-surfacing – be trapped on the cell surface by the antagonist (see Fig. 1). Indeed, the addition of exendin9-39 rapidly reversed the donor/acceptor ratios promoted by GLP-1 with a $t_{1/2\_rec}$ of 18.1 ± 1.2 min (at EC_{50} = 10 nM, Fig. 7A and Table 1). Similar to GLP-1, exendin-4- and liraglutide-induced GLP-1R internalized receptors were recycled in a concentration-dependent manner with $t_{1/2\_rec}$ of 51.2 ± 1.6 (at EC_{50} = 10 nM, Fig. 7B) and 64.7 ± 2.7 min (at EC_{50} = 100 nM, Fig. 7C) for exendin-4 and liraglutide, respectively (Table 1). Interestingly, the GLP-1R recycling rate after internalization induced by an EC_{50} concentration of GLP-1 was significantly faster than that compared to exendin-4 ($P < 0.001$) or liraglutide ($P < 0.001$). Since GLP-1 is not resistant to degrading enzymes such as DPP-4 (Kieffer et al., 1995), as opposed to exendin-4 and liraglutide, the faster $t_{1/2\_rec}$ observed for GLP-1 activated receptors could be caused by ligand degradation. In fact, a recycling experiment conducted in the presence of the DPP-4 inhibitor valpyr resulted in slower GLP-1 mediated GLP-1R recycling. Still, receptor recycling mediated by GLP-1was significantly faster compared to exendin-4 (Supplementary Fig. 5). As a control – and in agreement with previous findings by Widmann et al. in 1995 (Widmann et al., 1995) and our in vivo studies of GLP-1R internalization in pancreatic islets (Fig. 4B) – we also confirmed that the antagonist exendin9-39 did not induce GLP-1R internalization *per se* (Fig. 7D).

Since our microscopy studies indicated a prolonged co-localization of internalized receptors with early recycling endosomal markers (Fig. 5), we speculated that receptors would continue to be recycled even after prolonged activation by agonist. To examine this possibility, we repeated our real-time recycling experiment, but added an excess of exendin9-39 after 90 min of agonist-induced internalization. As was the case after only 20 min of activation (Fig. 7), antagonist addition at 90 min also rapidly reversed the donor/acceptor ratios promoted by GLP-1 (Fig. 8A, closed symbols) as well as exendin-4 (Fig. 8B, closed symbols) and liraglutide (Fig. 8C, closed symbols), indicating recycling of GLP-1R even after prolonged activation. Nevertheless, in the absence of antagonist, the plateau arising from prolonged agonist induced internalization

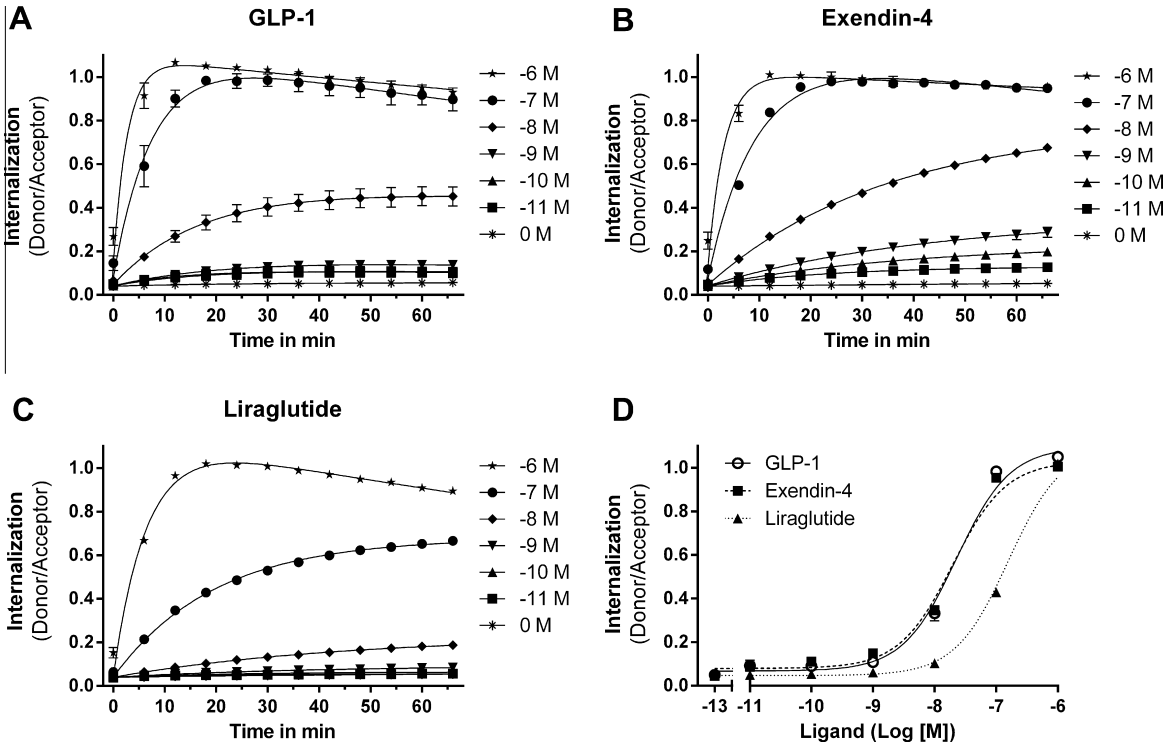

Fig. 6. Real-time internalization of GLP-1R. Surface expressed SNAP-GLP-1Rs were labeled with a cell-impermeable energy donor and cells were subsequently incubated in excess of energy acceptor. Cells were then stimulated with increasing concentrations of ligands and the internalization of GLP-1R was measured in real-time at 37 °C. Real-time internalization of GLP-1Rs in the presence of **(A)** GLP-1, **(B)** exendin-4, or **(C)** liraglutide is shown as increase in the donor/acceptor ratio as a function of time. **(D)** Concentration-response curves for the time point of maximum GLP-1R internalization (20 min) induced by GLP-1 (open circle, full line), exendin-4 (closed square, dashed line), or liraglutide (closed triangle, dotted line). Data represent mean ± SD from one representative out of three independent experiments carried out in triplicates. Data were plotted in GraphPad Prism and fitted to **(A–C)** a model based on a product of one phase association and one phase decay and **(D)** a log(agonist) vs. response model.

Table 1
Kinetics of ligand-induced GLP-1R internalization and recycling.

	GLP-1	Exendin-4	Liraglutide
$T_{1/2int}$ *(min)*			
−9M	18.1 ± 1.7	28.5 ± 0.3	21.2 ± 2.7
−8M	**11.6 ± 0.8**	**21.1 ± 1.7**	33.0 ± 1.3
−7M	4.8 ± 0.4	5.8 ± 0.5	**16.5 ± 2.0**
−6M	2.6 ± 0.4	2.7 ± 0.3	4.9 ± 0.4
$T_{1/2rec}$ *(min)*			
−9M	18.9 ± 1.8	57.1 ± 3.1	–
−8M	**18.1 ± 1.2**	**51.2 ± 1.6**	67.6 ± 5.4
−7M	16.1 ± 1.1	54.5 ± 0.6	**64.7 ± 2.7**
−6M	15.3 ± 1.2	32.6 ± 2.5	99.9 ± 2.3

Values are means ± SEM from three independent experiments carried out in triplicates. $T_{int} = \ln(2)/K_{int}$ (internalization rate constant). $T_{1/2rec} = \ln(2)/K_{rec}$ (recycling rate constant). Kinetic values at EC_{50} values corresponding to 12.0 ± 4.8 nM for GLP-1, 13.1 ± 3.6 nM for exendin-4, and 158 ± 22 nM for liraglutide are highlighted in bold.

declined over time following the maximum at ~20 min (Fig. 8, open symbols), suggesting that not all receptors are recycled.

Summarized, these data suggest that GLP-1R is efficiently recycled and that it recycles more rapidly upon stimulation with GLP-1 as compared to exendin-4 and liraglutide. In addition, GLP-1R recycling continues to occur even during prolonged activation.

3.7. Validation of TR-FRET based receptor internalization assay

In order to validate our findings that the GLP-1R is both a fast internalizing and recycling receptor, we compared the real-time trafficking properties of the GLP-1R to that of the β_2-adrenergic receptor (β_2AR), which is a prototypical internalizing and recycling receptor (von Zastrow and Kobilka, 1994). N-terminally SNAP-tagged β_2AR (SNAP-β_2AR) was transiently expressed in HEK293 cells and surface expressed receptors were labeled with SNAP lumi4®-Tb. Stimulation of the SNAP-β_2AR with the agonist isoproterenol induced receptor internalization at concentrations > 1 nM (Fig. 9A). In the absence of agonist, an increase in donor/acceptor ratio was observed. This increase likely reflects a degree of constitutive internalization of the β_2AR. Recycling of the SNAP-β_2AR was induced by adding an excess of the cell impermeable β_2AR antagonist sotalol following 30 min of agonist induced internalization. Addition of sotalol (Fig. 9B) resulted in a decreased donor/acceptor ratio as expected from receptors recycling back to the cell surface following agonist induced internalization.

Compared to the GLP-1R ($t_{1/2\_int}$ of 2.6 ± 0.4 min at 1 μM GLP-1), the kinetics of ligand-dependent β_2AR internalization ($t_{1/2\_int}$ of 12.9 ± 1.0 min at 100 nM isoproterenol) was significantly slower than that of the GLP-1R ($P < 0.001$). Similarly, when the recycling kinetics for β_2AR ($t_{1/2\_rec}$ of 28.6 ± 3.4 min at 100 nM isoproterenol) were compared to those of the GLP-1R ($t_{1/2\_int}$ of 15.3 ± 1.2 min at 1 μM GLP-1), the GLP-1R recycling was significantly faster compared to that of the β_2AR ($P < 0.05$). These data suggest that the GLP-1R is a fast internalizing and predominantly recycling receptor.

3.8. Slow post-endocytic degradation of GLP-1Rs

Upon prolonged agonist stimulated GLP-1R internalization, the plateau following the internalization maximum was observed to decline over time (Fig. 8, open symbols and Fig. 6, high concentrations). This decline was observed for all ligands tested, and we speculated that this might likely reflect some loss of receptor number over time.

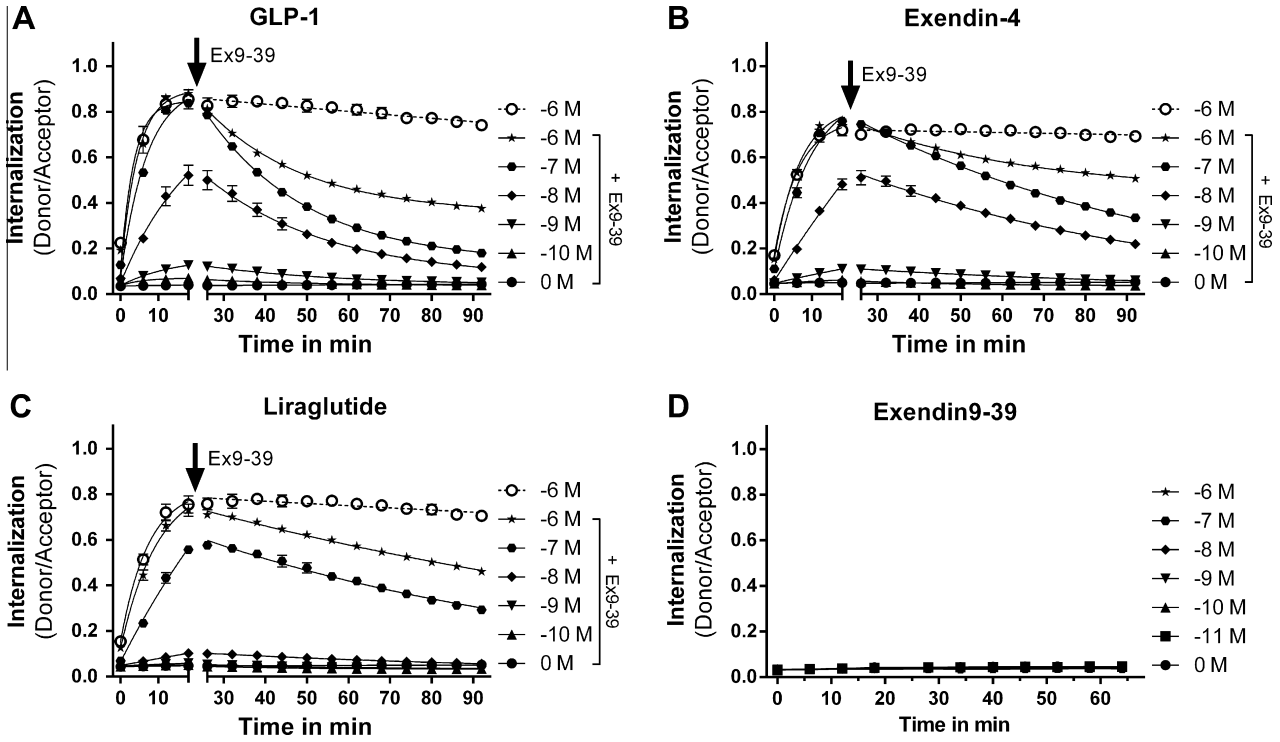

Fig. 7. Real-time recycling of GLP-1R. Internalization assays were performed as in Fig. 6. Following 20 min of GLP-1R internalization induced by **(A)** GLP-1, **(B)** exendin-4, or **(C)** liraglutide, an excess of 10 μM of exendin9-39 was added (indicated by arrow) to block further internalization and induce receptor recycling. Open symbols (circle, dashed line) represent GLP-1R internalization in the absence of exendin9-39 (ex9-39). Real-time internalization and recycling of GLP-1R are reflected by an increase and a decrease in donor/acceptor ratios, respectively, and plotted as a function of time. Data were fitted to a one phase association model (internalization phase) and a one phase decay model (recycling phase). **(D)** The antagonist exendin9-39 does not induce GLP-1R internalization *per se*. All data represent mean ± SD from one representative out of three independent experiments carried out in triplicates.

Thus, we next investigated whether internalized GLP-1Rs are – at least to some degree – degraded following prolonged ligand stimulation using a biotin protection and degradation assay. In this assay, surface expressed SNAP-GLP-1Rs were biotinylated for 30 min prior to stimulation with 100 nM of either GLP-1 (Fig. 10A), exendin-4 (Fig. 10B), liraglutide (Fig. 10C) or vehicle (Fig. 10A–C). Following stimulation for the time periods indicated, remaining surface-bound biotin was stripped off and the internalized protected pool of receptors was immunoprecipitated with SNAP-tag antibody and immunoblotted against biotin. The loss of receptors was quantified against the total amount of internalized receptors at 15 min (Fig. 10D–F), which corresponds to the approximated time of maximal GLP-1R internalization (Fig. 6). In the presence of GLP-1 (Fig. 10A and D), internalized GLP-1Rs were slowly degraded with a $t_{1/2\_deg}$ of 133.6 ± 2.3 min. Following 120 min post-ligand stimulation, 41 ± 4% receptors were still not degraded. Similarly, exendin-4 (Fig. 10B and E) induced a slow ($t_{1/2\_deg}$ of 129.6 ± 20.1 min) and partial (54 ± 12% following 120 min stimulation) GLP-1R degradation. Upon stimulation with liraglutide (Figs. 10C and F), internalized GLP-1Rs degraded with a $t_{1/2\_deg}$ of 85.4 ± 5.3 min resulting in 29 ± 5% non-degraded internalized receptors following 120 min stimulation. These results show a tendency towards GLP-1R degradation being marginally faster in response to liraglutide as compared to GLP-1. However, no significant variances in the receptor degradation endpoint levels or degradation rates were found comparing the three ligands.

These data are in line with our real time internalization assays, i.e. following maximum receptor internalization at 15–20 min, the internalization plateau starts to steadily decline in the presence of prolonged agonist stimulation. These data suggest that GLP-1R is a mainly recycling receptor, however, a proportion of the internalized receptor pool is slowly degraded over time for all ligands tested.

4. Discussion

Here we investigated the trafficking and signaling properties of GLP-1R in real time in response to its natural ligand GLP-1 and the two stable analogues exendin-4 and liraglutide. Specifically, we combined novel real-time measurements of internalization and cAMP signaling in living cells to determine the kinetics of GLP-1R internalization, recycling and signaling. We found that GLP-1R undergoes rapid internalization in the presence of the human incretin hormone GLP-1 in correspondence with previous publications (Widmann et al., 1995; Jorgensen et al., 2007; Kuna et al., 2013). In addition, we found equally fast internalization rates of GLP-1R in the presence of exendin-4 and liraglutide at equipotent concentrations (Fig. 6). The fast kinetics of GLP-1R internalization simultaneous with its ligands was confirmed in microscopy studies (Fig. 3). Furthermore, the biological significance of GLP-1R internalization was demonstrated in vivo. We here show that both a fluorescently labeled GLP-1 agonist as well as an antagonist can readily label GLP-1Rs in mouse pancreatic islets (Fig. 4). This labeling was specific for the mode of action of the ligand, i.e. the antagonist exendin9-39 inactivates and labels GLP-1Rs on the surface of β-cells in the pancreatic islets, whereas the agonist exendin-4 accumulates in intracellular compartments, suggesting GLP-1R internalization as an important characteristic of activated endogenously expressed receptors.

We found that GLP-1R following internalization readily recycles in response to all agonists tested (Fig. 7). Moreover, the receptor even recycles after prolonged agonist treatment (Fig. 8). This was shown by i) the ability to measure GLP-1R recycling at a very late

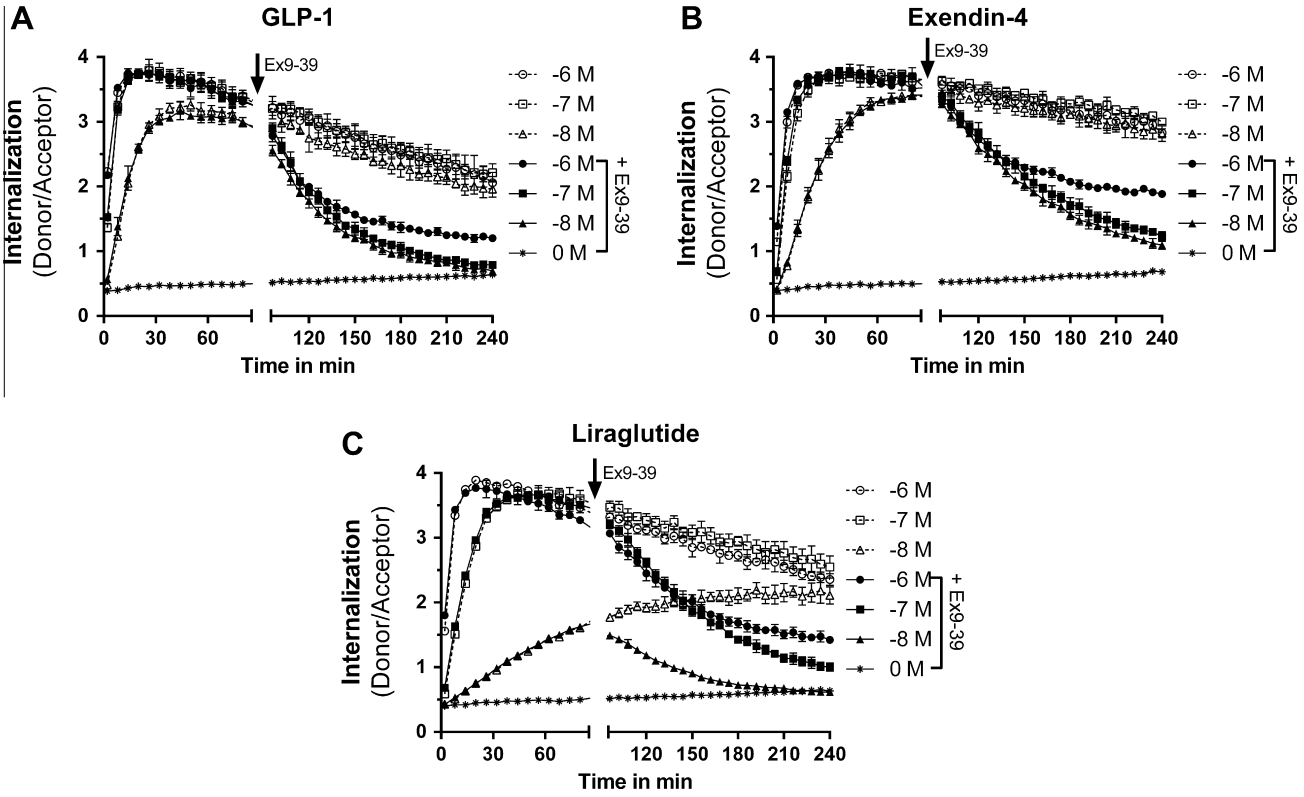

Fig. 8. Prolonged GLP-1R recycling. Internalization assays were performed as in Fig. 6. Following 90 min of GLP-1R internalization induced by **(A)** GLP-1, **(B)** exendin-4, or **(C)** liraglutide, an excess of 10 μM of exendin9-39 (indicated by arrow) was added to block further internalization and induce receptor recycling (closed symbols, full lines). Open symbols (dashed lines) represent GLP-1R internalization in the absence of exendin9-39. Real-time internalization and recycling of GLP-1R are reflected by an increase and a decrease in donor/acceptor ratios, respectively, and plotted as a function of time. All data represent mean ± SD from one representative out of two independent experiments carried out in triplicates.

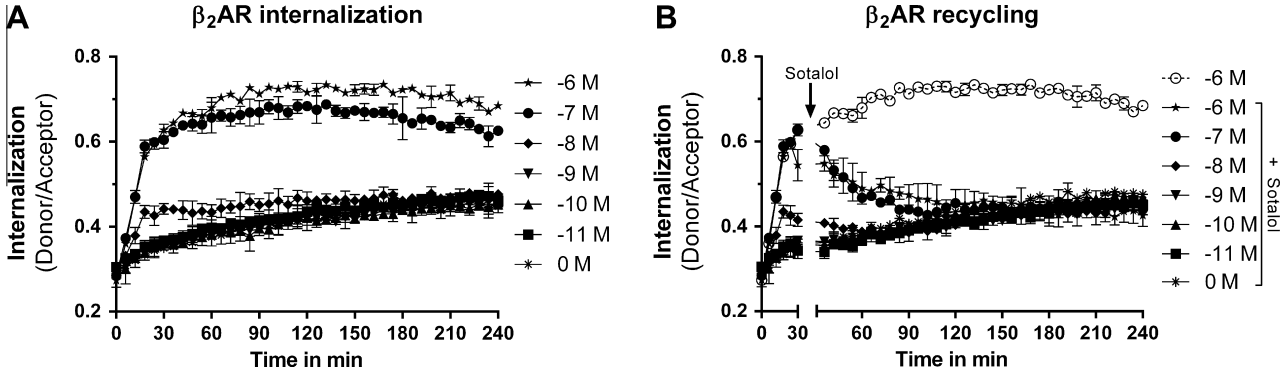

Fig. 9. Real-time internalization and recycling of β_2AR. HEK293 cells were transiently transfected with SNAP-β_2AR plasmid and used for internalization and recycling assays as described in Figs. 6 and 7. **(A)** Internalization was initiated by stimulation of β_2AR with isoproterenol. **(B)** For recycling experiments, an excess of 10 μM of sotalol (indicated by arrow) was added following 30 min of agonist stimulation to block further internalization and induce receptor recycling (closed symbols, full lines). Open symbols (circle, dashed line) represent receptor internalization in the absence of antagonist. Real-time internalization and recycling of β_2AR are reflected by an increase and a decrease in donor/acceptor ratios, respectively, and plotted as a function of time. All data represent mean ± SD from one representative out of three independent experiments carried out in duplicates.

time point following agonist stimulation (Fig. 8) and by ii) a prolonged co-localization of GLP-1Rs with recycling endosomal markers for up to 60 min (Fig. 5). Interestingly, GLP-1R recycling was 2–3 times slower when induced by exendin-4 and liraglutide as compared to GLP-1 at equipotent concentrations. These differences correspond with a longer co-localization found between GLP-1Rs and recycling endosomes in the presence of exendin-4 and liraglutide as opposed to GLP-1 (Fig. 5). Ligand dependent recycling variances can be speculated to be caused by differences in the on/off rates of ligand binding to GLP-1R. For instance, a prolonged ligand binding to GLP-1R might keep the receptor in the recycling loop for a longer time period. Whether the decreased recycling rates – possibly by such a prolonged receptor-ligand constellation – may partially be accountable for the prolonged half-life and improved blood glucose control of liraglutide and exendin-4 in the clinics has yet to be elucidated.

The utility of the novel TR-FRET based assay to study both internalization and recycling of the GLP-1R was confirmed by comparing the kinetics of the GLP-1R to that of the β_2AR (Fig. 9), a prototypical internalizing and recycling receptor (von Zastrow

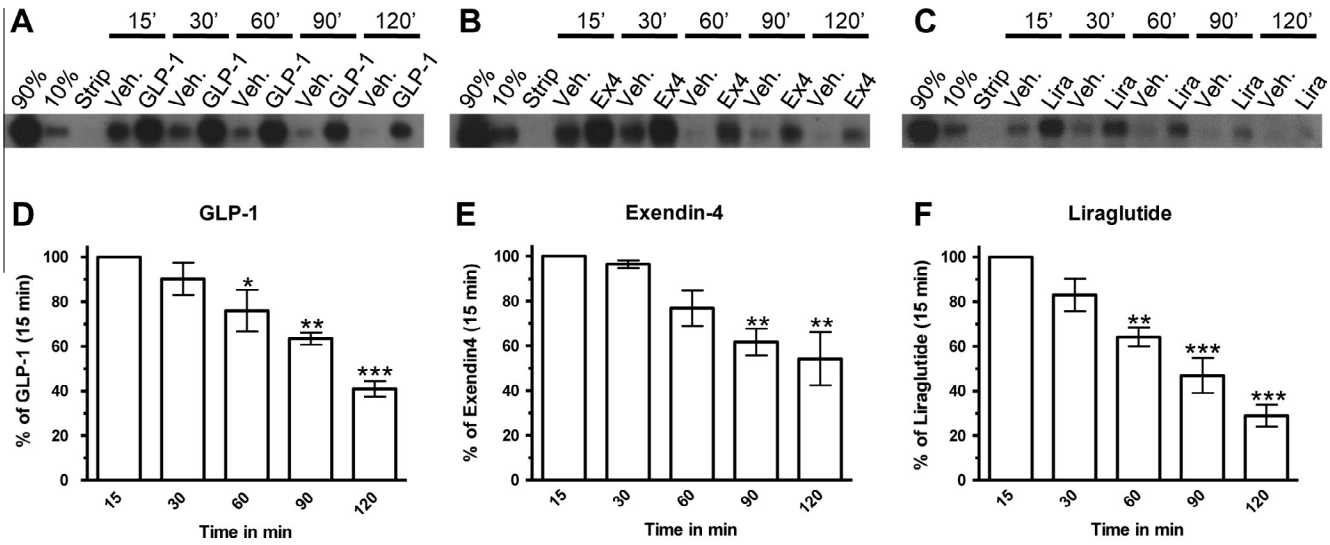

Fig. 10. Slow degradation of internalized GLP-1Rs. Surface expressed SNAP-GLP-1Rs were biotinylated (A–C, lanes 90% and 10%) and either stripped (A-C, Strip lanes) or treated with cell culture medium as vehicle (A–C, Veh. = vehicle) or 100 nM of **(A)** GLP-1, **(B)** exendin-4 (Ex4) or **(C)** liraglutide (lira) for the time periods indicated. Then cells were stripped and the "protected" internalized receptor pool was immunoprecipitated with anti-SNAP antibody and immunoblotted against biotin. **(D–F)** Quantification of multiple experiments performed in A–C with receptor degradation expressed as percentage of internalized receptors at 15 min after ligand stimulation. Data represents mean ± SEM from four independent experiments. A one-way ANOVA with Dunnett's post-test was used to compare degradation for each time point to receptor levels at 15 min in GraphPad Prism; $^{*}P < 0.05$, $^{**}P < 0.01$, $^{***}P < 0.001$.

and Kobilka, 1994). Stimulation of the β_2AR with isoproterenol induced receptor internalization in a concentration dependent manner. Likewise, addition of the antagonist sotalol resulted in a decrease in the donor/acceptor ratio, reflecting recycling of β_2AR. Interestingly, both the internalization and recycling rates of GLP-1R were significantly faster compared to those measured for the β_2AR.

The recycling rate of GLP-1R could possibly be influenced by differences in receptor degradation rates induced by GLP-1, exendin4, and liraglutide. However, this was ruled out, since no significant differences in receptor degradation rates comparing the three ligands were detected in the biotinylation degradation studies (Fig. 10). In fact, all three ligands tested stimulated slow and partial receptor degradation. This slow degradation is furthermore reflected by a drop in the internalization plateaus following prolonged ligand stimulation (Fig. 8). Taken together, our data suggest that a pool of GLP-1Rs is sorted to degradation following prolonged agonist stimulation, while the majority of receptors continue to recycle. Slow receptor degradation may likely be part of a cell self-defense mechanism in response to chronic treatment where an overall receptor downregulation is initiated in order to protect against overstimulation.

While degradation ultimately leads to signal termination, recycling is classically linked to resensitization (Hanyaloglu and von Zastrow, 2008). We have shown that GLP-1Rs rapidly and repeatedly internalize and recycle upon ligand activation. Thus, one could anticipate a prolonged signaling from GLP-1Rs caused by continuous receptor recycling and resensitization. Indeed, when measuring the real-time cAMP production induced by GLP-1R activation, we found an immediate increase in cAMP levels followed by a prolonged signaling plateau for GLP-1 as well as exendin-4 and liraglutide (Fig. 2). Similar to the prolonged signaling from GLP-1R shown here, results from Mathiesen et al. (2013) suggest a prolonged signaling from activated β_2AR expressed at high levels. In contrast, cAMP signaling from β_2AR expressed at endogenous level was fast and transient. Thus, it can be speculated that a prolonged signal is caused by the presence of excess of receptors and the inability of the intracellular machinery to desensitize the receptors. As anticipated, the addition of an antagonist following agonist stimulated cAMP production rapidly decreases the cAMP signal, i.e. due to both the i) inactivation of receptors on the cell surface and ii) trapping and inactivating of receptors once they are recycled back to the cell surface.

In conclusion, we have utilized a novel TR-FRET based technique to show that the human GLP-1R internalizes fast and with similar kinetics in response to GLP-1, exendin-4, and liraglutide. In contrast, the rate of GLP-1R recycling is slower for liraglutide and exendin-4 when compared to GLP-1. Independent of the ligand, activated GLP-1Rs were shown to cycle for a prolonged period of time as well as exhibiting a prolonged cAMP signal. Recently, a study by Kuna et al. (2013) even suggests a direct link between internalized GLP-1Rs and prolonged cAMP signaling in line with recent results from Irannejad et al. showing signaling from internalized GPCRs (Irannejad et al., 2013). Here, we suggest that prolonged cAMP signaling might be correlated to a continuous cycling and resensitization of GLP-1Rs following activation with an agonist, thereby emphasizing the importance of studying the post-endocytic trafficking properties of this prominent drug target.

Acknowledgements

We wish to thank Eric Trinquet and Hamed Mokrane from Cisbio Bioassays for invaluable help on optimizing the TR-FRET based real-time internalization assay. In addition, the authors are grateful to Barbara Maurer and Trine Lind Devantier from Department of Incretin & Islet Biology, Novo Nordisk A/S, Maaloev, Denmark for helping generating the stable cell line used in this study; Maria Fè Lanfranco Gallofrè and Johan Enquist of the Ernest Gallo Clinic and Research Center, Department of Neurology, University of California San Francisco, for assisting with the biotinylation protection degradation assay. Author contributions: S.N.R. and M.W. designed research; S.N.R., P.W., C.R.U., H.I., K.A.C., J.L., J.H.S., and A.S. performed research; S.M.K., L.S., J.M.M., H.B.-O., and N.K. contributed new reagents/analytic tools; S.N.R., N.K., J.W., and M.W. analyzed data; S.N.R. and M.W. wrote the paper. J.M.M. and H.B.-O. were supported by grants from the Lundbeck Foundation and the Danish Council for Independent Research Medical Sciences.

Appendix A. Supplementary material

Supplementary data associated with this article can be found, in the online version, at http://dx.doi.org/10.1016/j.mce.2013.11.010.

References

Cisbio Bioassays, 2012. Ref Type: Online Source<http://www.cisbio.com/>.

Göke, R., Fehmann, H.C., Linn, T., Schmidt, H., Krause, M., Eng, J., Göke, B., 1993. Exendin-4 is a high potency agonist and truncated exendin-(9-39)-amide an antagonist at the glucagon-like peptide 1-(7-36)-amide receptor of insulin-secreting beta-cells. J. Biol. Chem. 268, 19650–19655.

Grant, B.D., Donaldson, J.G., 2009. Pathways and mechanisms of endocytic recycling. Nat. Rev. Mol. Cell. Biol. 10, 597–608.

Hanyaloglu, A.C., von Zastrow, M., 2008. Regulation of GPCRs by endocytic membrane trafficking and its potential implications. Annu. Rev. Pharmacol. Toxicol. 48, 537–568.

Holst, J.J., 2007. The physiology of glucagon-like peptide 1. Physiol. Rev. 87, 1409–1439.

Irannejad, R., Tomshine, J.C., Tomshine, J.R., Chevalier, M., Mahoney, J.P., Steyaert, J., Rasmussen, S.G., Sunahara, R.K., El-Samad, H., Huang, B., von, Z.M., 2013. Conformational biosensors reveal GPCR signalling from endosomes. Nature.

Jorgensen, R., Kubale, V., Vrecl, M., Schwartz, T.W., Elling, C.E., 2007. Oxyntomodulin differentially affects glucagon-like peptide-1 receptor beta-arrestin recruitment and signaling through Galpha(s). J. Pharmacol. Exp. Ther. 322, 148–154.

Kieffer, T.J., McIntosh, C.H., Pederson, R.A., 1995. Degradation of glucose-dependent insulinotropic polypeptide and truncated glucagon-like peptide 1 in vitro and in vivo by dipeptidyl peptidase IV. Endocrinology 136, 3585–3596.

Kuna, R.S., Girada, S.B., Asalla, S., Vallentyne, J.S.M., Patterson, J.T., Smiley, D.L., Dimarchi, R.D., Mitra, P., 2013. Glucagon-like peptide1 receptor mediated endosomal CAMP generation promotes glucose stimulated insulin secretion in pancreatic beta cells. Am. J. Physiol. Endocrinol. Metab..

Martini, L., Waldhoer, M., Pusch, M., Kharazia, V., Fong, J., Lee, J.H., Freissmuth, C., Whistler, J.L., 2007. Ligand-induced down-regulation of the cannabinoid 1 receptor is mediated by the G-protein-coupled receptor-associated sorting protein GASP1. FASEB J. 21, 802–811.

Mathiesen, J.M., Vedel, L., Bräuner-Osborne, H., 2013. CAMP biosensors applied in molecular pharmacological studies of G protein-coupled receptors. Methods Enzymol. 522, 191–207.

Maurel, D., Comps-Agrar, L., Brock, C., Rives, M.L., Bourrier, E., Ayoub, M.A., Bazin, H., Tinel, N., Durroux, T., Prézeau, L., Trinquet, E., Pin, J.P., 2008. Cell-surface protein-protein interaction analysis with time-resolved FRET and snap-tag technologies: application to GPCR oligomerization. Nat. Methods 5, 561–567.

Mayo, K.E., Miller, L.J., Bataille, D., Dalle, S., Goke, B., Thorens, B., Drucker, D.J., 2003. International union of pharmacology. XXXV The glucagon receptor family. Pharmacol. Rev. 55, 167–194.

Meier, J.J., 2012. GLP-1 receptor agonists for individualized treatment of type 2 diabetes mellitus. Nat. Rev. Endocrinol. 8, 728–742.

Meier, J.J., Nauck, M.A., 2010. Is the diminished incretin effect in Type 2 diabetes just an Epi-phenomenon of impaired beta-cell function? Diabetes 59, 1117–1125.

Ponsioen, B., Zhao, J., Riedl, J., Zwartkruis, F., van der Krogt, G., Zaccolo, M., Moolenaar, W.H., Bos, J.L., Jalink, K., 2004. Detecting CAMP-induced Epac activation by fluorescence resonance energy transfer: Epac as a novel CAMP indicator. EMBO Rep. 5, 1176–1180.

Tsao, P., Cao, T., von Zastrow, M., 2001. Role of endocytosis in mediating downregulation of G-protein-coupled receptors. Trends Pharmacol. Sci. 22, 91–96.

Tschische, P., Moser, E., Thompson, D., Vischer, H.F., Parzmair, G.P., Pommer, V., Platzer, W., Schwarzbraun, T., Schaider, H., Smit, M.J., Martini, L., Whistler, J.L., Waldhoer, M., 2010. The G-protein coupled receptor associated sorting protein GASP-1 regulates the signalling and trafficking of the viral chemokine receptor US28. Traffic 11, 660–674.

von Zastrow, M., Kobilka, B.K., 1994. Antagonist-dependent and -independent steps in the mechanism of adrenergic receptor internalization. J. Biol. Chem. 269, 18448–18452.

Whistler, J.L., Enquist, J., Marley, A., Fong, J., Gladher, F., Tsuruda, P., Murray, S.R., von Zastrow, M., 2002. Modulation of postendocytic sorting of G protein-coupled receptors. Science 297, 615–620.

Widmann, C., Dolci, W., Thorens, B., 1995. Agonist-induced internalization and recycling of the glucagon-like peptide-1 receptor in transfected fibroblasts and in insulinomas. Biochem. J. 310, 203–214.

Widmann, C., Dolci, W., Thorens, B., 1996a. Desensitization and phosphorylation of the glucagon-like peptide-1 (GLP-1) receptor by GLP-1 and 4-phorbol 12-myristate 13-acetate. Mol. Endocrinol. 10, 62–75.

Widmann, C., Dolci, W., Thorens, B., 1996b. Heterologous desensitization of the glucagon-like peptide-1 receptor by phorbol esters requires phosphorylation of the cytoplasmic tail at four different sites. J. Biol. Chem. 271, 19957–19963.

Widmann, C., Dolci, W., Thorens, B., 1997. Internalization and homologous desensitization of the GLP-1 receptor depend on phosphorylation of the receptor carboxyl tail at the same three sites. Mol. Endocrinol. 11, 1094–1102.